JOURNAL OF SOLID STATE CHEMISTRY 40, 361–368 (1981)

^{2}D and ^{133}Cs NMR Study of the Hydrogen Bond Network and Antiferroelectric Phase Transition of Cesium Trihydrogen Selenite

I. S. VINOGRADOVA

L. V. Kirensky Institute of Physics Academy of Sciences, USSR Siberian Branch Krasnoyarsk, 660036, USSR

Received March 20, 1981; in revised form August 10, 1981

The ^{2}D and ^{133}Cs NMR spectra of deuterated and protiated single crystals of antiferroelectric cesium trihydrogen selenite have been studied in the high- and low-temperature phases. The number of chemically nonequivalent hydrogen bonds, their lengths, and directions in the unit cell were determined from deuteron electric field gradient tensors. The deuterons of centered hydrogen bonds have been found disordered in the paraelectric phase over two equivalent sites on either side of a center of symmetry. The antiferroelectric phase transition is accompanied by order–disorder phenomena of the H system and displacive behavior of the heavy-ion system.

$CsH_3(SeO_3)_2$ belongs to the family of alkali trihydrogen selenites and shows antiferroelectric properties below $-128°C$ [*1*]. Although the literature on these crystals is quite extensive, little in known about cesium trihydrogen selenite (CTHS), its properties and the nature of its phase transition.

The crystal structure of the paraelectric phase of CTHS was studied by Sato [*2*] and Tellgren and co-workers [*3, 4*]. Two formula units crystallize in a triclinic unit cell with centrosymmetric space group $P\bar{1}$. The heavy atom unit consists of a Cs^{+} ion and two SeO_3 groups linked via hydrogen bonds. There are five nonequivalent hydrogen bonds, four of them lie across centers of symmetry. The position of the protons were found by two-dimensional neutron diffraction data [*2*] and by three-dimensional single-crystal X-ray [*3*] and neutron diffraction [*4*] data. The disordered-hydrogen-atoms model was assumed in these papers for centered hydrogen bonds. The low-temperature structure data are absent.

In the phase transition range, dielectric, optical, thermal, and pyroelectric properties were studied by Makita [*1*]; ir spectra by Khanna *et al.* [*5*]. The results of these few investigations do not permit one to describe fully the phase transition. A large effect of deuteration on the transition temperature found by Gavrilova–Podolskaya *et al.* [*6*] indicates an order–disorder transition with a significant role of hydrogen-bonded protons in the phase transition mechanism. Sato, Khanna *et al.*, and Tellgren have suggested that the paraelectric phase contains disordered configurations of H_2SeO_3 and $HSeO_3^{-}$ and the transition to the antiferroelectric phase is accompanied by an ordering of the hydrogen atoms.

In this paper, in order to elucidate the phase transition mechanism, the role of hydrogen bonds, and the heavy-atom system,

0022-4596/81/150361-08$02.00/0

^{2}D and ^{133}Cs NMR spectra of the deuterated (CTDS) and protiated (CTHS) single crystals were studied.

Experimental

Cesium trideuterium selenite was synthesized by the reaction of SeO_2 with Cs_2CO_3 in D_2O. Single crystals were grown by gradual evaporation of a solution of this compound in D_2O. As determined from the dielectric constant and ^{133}Cs spectra measurements, the transition temperature T_c was found to be −90°C. The ^{2}D and ^{133}Cs NMR spectra were recorded in a magnetic field about 13 kG. Angular dependences of the first-order quadrupole splittings of the spectra were measured for crystal rotation about three mutually orthogonal axes in both phases. The rotation axes were defined as follows: the Z axis is taken to be parallel to the crystallographic c axis; the X axis, in the (010) plane perpendicular to the c axis; and the Y axis, perpendicular to the X and Z axes. From the rotation patterns, the principal values and the direction cosines of the electric field gradient (EFG) tensors, the values of the guadrupole coupling constant eQq/h, and the asymmetry parameter η were determined by the Volkoff method [7]. The results are tabulated in Tables I–III. The estimated errors in the principal values are about ±2 kHz; the error in angle is within ±2°.

TABLE I

PRINCIPAL VALUES AND DIRECTION COSINES OF THE PRINCIPAL AXES OF THE ^{2}D FIELD GRADIENT TENSORS IN CESIUM TRIHYDROGEN SELENITE

	eQq_u/h (kHz)	Direction cosines with respect to X	Y	Z
Paraelectric phase (+15°C)				
D(1)	56.8	+0.6441	−0.1903	+0.7647
	77.5	−0.1319	+0.9819	+0.1356
	134.3	+0.7535	+0.1882	−0.6299
D(2)	61.9	+0.0461	+0.9421	−0.3321
	79.8	−0.3794	+0.3240	+0.8660
	141.7	+0.9241	+0.0861	+0.3724
D(3)	58.8	−0.4034	+0.5483	+0.7325
	79.6	+0.6099	+0.7579	−0.2314
	138.4	+0.6821	−0.3534	+0.6402
D(4)	61.9	+0.2190	+0.9757	−0.0078
	73.5	+0.9700	−0.2185	−0.1066
	135.5	+0.1057	−0.0157	+0.9942
D(5)	55.9	+0.6373	+0.3315	+0.6959
	79.4	+0.2652	+0.7532	−0.6019
	135.4	+0.7235	−0.5681	−0.3922
Antiferroelectric phase (−125°C)				
$D(1)_a$	50.9	+0.6006	+0.0602	+0.7972
	74.4	−0.2164	+0.9722	+0.0896
	125.4	+0.7696	+0.2264	−0.5969
$D(1)_b$	46.2	+0.6101	+0.0347	+0.7915
	71.7	−0.1238	+0.9909	+0.0519
	117.9	+0.8726	+0.1297	−0.6089
D(2)	67.6	+0.0274	+0.9658	−0.2578
	87.8	−0.3764	+0.2488	+0.8924
	155.5	+0.9260	+0.0726	+0.3704
D(3)	64.8	+0.4216	−0.5732	−0.7026
	90.5	+0.6143	+0.7507	−0.2437
	155.3	+0.6670	−0.3288	+0.6686
D(4)	67.5	+0.1928	+0.9806	−0.0348
	82.6	+0.9773	−0.1961	−0.0822
	150.2	+0.0874	+0.0182	+0.9960
D(5)	65.2	+0.6510	+0.3889	+0.6518
	87.5	+0.2273	+0.7194	−0.6463
	152.7	+0.7242	−0.5755	−0.3799

Results

Deuteron Magnetic Resonance

Five pairs of DMR absorption lines were observed in the paraelectric phase. Four pairs of lines D(2)–D(5) are of nearly equal intensity and one pair of lines D(1) was about two times as intense as the lines D(2)–D(5). Figure 1 shows the rotation patterns of the DMR absorption lines at +15°C (dotted lines). According to the DMR data there are five chemically nonequivalent sites in the triclinic unit cell of CTDS corresponding to the five strong hydrogen bonds proposed from X-ray and ND studies. Calculated from eQq/h values in connection with [8], the lengths of the hydrogen bonds are in the range 2.51–2.53 Å (X-ray data 2.54–2.58 Å) (Table II). Each EFG tensor was assigned to an individual hydrogen atom in the hydrogen bond system O(1) . . . O(6) or O(i) . . . O(i)′ (i = 2, 3, 4, 5) by means of the empirical relation that the

TABLE II

EXPERIMENTAL DATA[a]

	eQq/h (kHz)	η	R (O. . .O) Å X-Ray	R (O. . .O) Å DMR	φ_z (°)	φ_y (°)	α_z (°)	α_y (°)	Assignment
Paraelectric phase (+15°C)									
D(1)	134.3	0.15	2.582	2.51	3	2			O(1)–D(1). . .O(6)
						42			O(1). . .D(1)–O(6)
D(2)	141.7	0.13	2.577	2.53	4	7			O(2). . .D(2). . .O(2)′
D(3)	138.4	0.15	2.546	2.52	2	2			O(3). . .D(3). . .O(3)′
D(4)	135.5	0.09	2.573	2.52	3	5			O(4). . .D(4). . .O(4)′
D(5)	135.4	0.17	2.561	2.52	5	3			O(5). . .D(5). . .O(5)′
Antiferroelectric phase (−125°C)									
$D(1)_a$	125.4	0.19	—	2.50			3	5	
$D(1)_b$	117.9	0.22	—	2.48			4	5	
D(2)	155.5	0.13	—	2.56			1	5	
D(3)	155.3	0.17	—	2.56			2	1	
D(4)	150.2	0.10	—	2.55			1	2	
D(5)	152.7	0.15	—	2.55			1	4	

[a] Deuteron quadrupole coupling constants eQq/h, asymmetry parameters η, assignments of the field gradient tensors to the hydrogen bond system, and hydrogen bond lengths of $CsD_3(SeO_3)_2$. Angles φ_z are between the q_{zz} directions and the assigned hydrogen bond O . . . O directions, angles φ_y are between the q_{yy} directions and the calculated directions perpendicular to the Se-O . . . O plane. Angles α_z are between q_{zz} directions in para- and antiferroelectric phases, angles α_y are between the q_{yy} directions in para- and antiferroelectric phases.

TABLE III

PRINCIPAL VALUES AND DIRECTION COSINES OF THE PRINCIPAL AXES OF THE ^{133}Cs FIELD GRADIENT TENSORS IN CESIUM TRIHYDROGEN SELENITE

	Temp. (°C)	eQq_{ii}/h (kHz)	Direction cosines with respect to X	Y	Z
$CsH_3(SeO_3)_2$	+18	308	+0.7169	−0.0006	+0.6971
		167	−0.1722	+0.9691	+0.1763
		141	−0.6755	−0.2464	+0.6949
	−101	325	+0.7234	−0.0306	+0.6897
		201	+0.2964	+0.9160	−0.2702
		124	−0.6235	+0.3999	+0.6717
Cs(1)	−144	375	+0.7128	+0.0535	+0.6993
		240	+0.3486	+0.8382	−0.4194
		135	−0.6086	+0.5427	+0.5788
Cs(2)	−144	284	+0.7176	−0.0438	+0.6951
		196	+0.0347	+0.9990	+0.0273
		88	−0.6959	+0.0047	+0.7184
$CsD_3(SeO_3)_2$	+18	313	+0.7110	−0.0470	+0.7010
		183	−0.3010	+0.8811	+0.3641
		130	−0.6348	−0.4705	+0.6120

principal Z axis of the EFG tnesor is nearly parallel to the hydrogen bond direction. The notation of the oxygen atoms are those labeled by Sato and Tellgren and coworkers. The deuterons D(2)–D(5) lie in hydrogen bonds O(2) . . . O(2)′ O(3) . . . O(3)′, O(4) . . . O(4)′, O(5) . . . O(5)′ crossing the symmetry centers (Fig. 2). It is possible for these bonds to have central location of the deuterons in a symmetrical single-minimum potential or disordered location in a double-minimum potential. So far as the quadrupole coupling constant value is related to the length of the hydrogen bond and the deuteron position in this bond, we can distinguish between these two cases from the DMR data. From eQq/h values [8] the estimated D . . . O distances are 1.47–1.50 Å when O . . . O distances are 2.5–2.6 Å. Thus, deuterons D(2)–D(5) are located not in the center of the bonds

but are displaced and therefore must be disordered to keep the center of symmetry of the cell.

Conflicting results relative to the position of D(1) deuterons in hydrogen bonds O(1) . . . O(6) were obtained in [2, 4] by the ND method. According to Sato, protons H(1) are ordered and lie in an asymmetric single-minimum position near O(1). Tellgren and co-workers concluded that the bonds O(1) . . . O(6) are also disordered and H(1) atoms are unequally distributed over two possible sites, the site closer to O(1) being the more occupied. The DMR results agree with the Sato data. The D(1) deuterons need to localize near O(1) in an asymmetric single-minimum potential in accordance with the values of the φ_y angles (Table II).

On the whole, the DMR data for paraelectric phase CTDS confirm the X-ray and ND structures of CTHS [2–4] and show evidence that protiated and deuterated crystals are isomorphous.

On going through the Curie point, the resonance line D(1) splits into two $D(1)_a$ and $D(1)_b$, but the number of D(2)–D(5) resonance lines does not change below T_c and, in the low-temperature phase, the DMR spectra consist of six pairs of lines of nearly equal intensity. The angular dependences of the spectral splitting in the ordered phase were measured at −125°C and

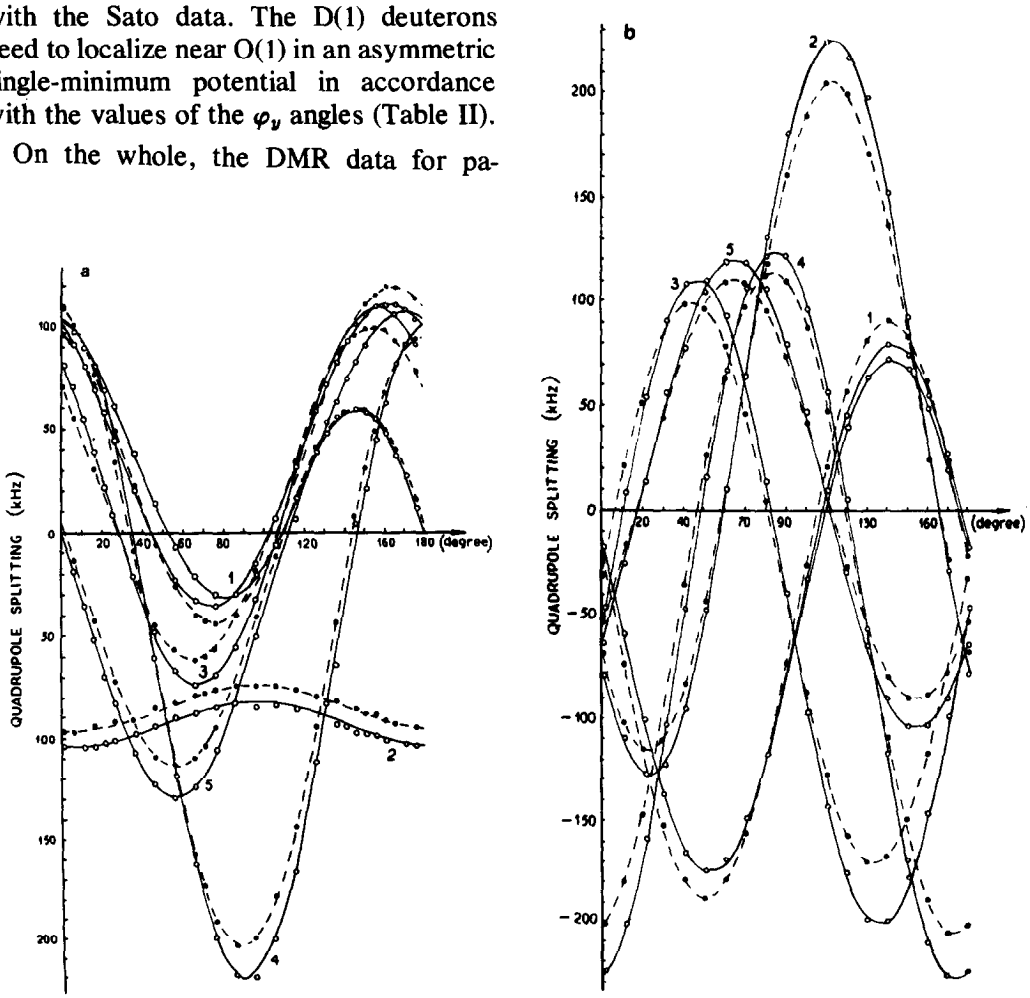

FIG. 1. Rotation patterns of the DMR absorption lines of $CsD_3(SeO_3)_2$. Solid curves indicate the antiferroelectric phase (−125°C), dotted lines signify the paraelectric phase (+15°C) (a) $H_0 \perp X$, $\theta_x = <Y, H_0$; (b) $H_0 \perp Y$, $\theta_y = <Z, H_0$; (c) $H_0 \perp Z$, $\theta_z = <X, H_0$.

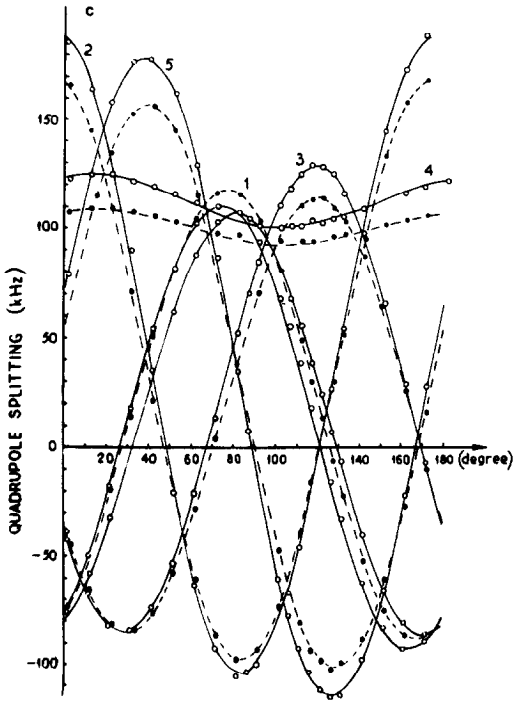

FIG. 1.—*Continued.*

are given in Fig. 1 by solid curves. They correspond to six nonequivalent hydrogen bonds. The lengths of these bonds are given in Table II together with α_z angles characterizing the change of their directions at the phase transition. The directions q_{zz} and q_{yy}, principal axes of the EFG tensors, vary within 5°.

^{133}Cs Magnetic Resonance

^{133}Cs magnetic resonance has been studied in CTHS and CTDS crystals. The ^{133}Cs nucleus has a high nuclear spin ($I = \frac{7}{2}$) and the quadrupole-split spectrum consists of seven equally spaced lines for each nonequivalent Cs^+ ion in the unit cell. The angular dependences of the first-order quadrupole splitting between the two $\pm\frac{3}{2} \leftrightarrow \pm\frac{1}{2}$ ^{133}Cs transitions in CTHS have been measured for crystal rotation about X, Y, Z axes in the paraelectric phase at +18°C and −101°C and in the antiferroelectric phase at −144°C ($T_c = -126$°C). In CTDS crystal, the temperature dependence of $2\Delta\nu$ has been measured with the specimen oriented so that the magnetic field lies in the (010) plane and makes an angle of 50° with the c axis (H_0 is nearly parallel to q_{zz}), $T_c = -90$°C. The results are given in Figs. 3 and 4.

In the paraelectric phase, two Cs^+ ions of the centrosymmetric unit cell are equivalent and the measured angular dependences correspond to one EFG tensor. Its principal values and direction cosines are given in Table III. At room temperature, the quadrupole coupling constant for protiated compound is equal to 308 ± 2 kHz and increases to 326 ± 2 kHz at −101°C. In the antiferroelectric phase, each satellite line splits into two and the observed spectrum of ^{133}Cs at −144°C is a superposition of the two quadrupole-split spectra. The angular dependences $2\Delta\nu$ in the ordered phase are given in Fig. 3. They correspond to two nonequivalent Cs sites in the unit cell with quadrupole coupling constant values of 284 ± 3 kHz and 375 ± 3 kHz. These results are in agreement with the crystallographic predictions of Sato and Makita, according to whom the centers of symmetry in the middle of the O . . . O bonds disappear below T_c, and the unit cell doubles along the c axis. Two Cs^+ ions of the initial unit cell become nonequivalent in the ordered phase, them correspond two EFG tensors (Table III). The doubled unit cell of the low-temperature phase is triclinic centro-

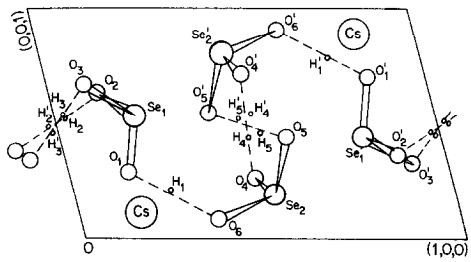

FIG. 2. A projection of the crystal structure of $CsH_3(SeO_3)_2$ on the (010) plane. Dotted lines indicate hydrogen bonds.

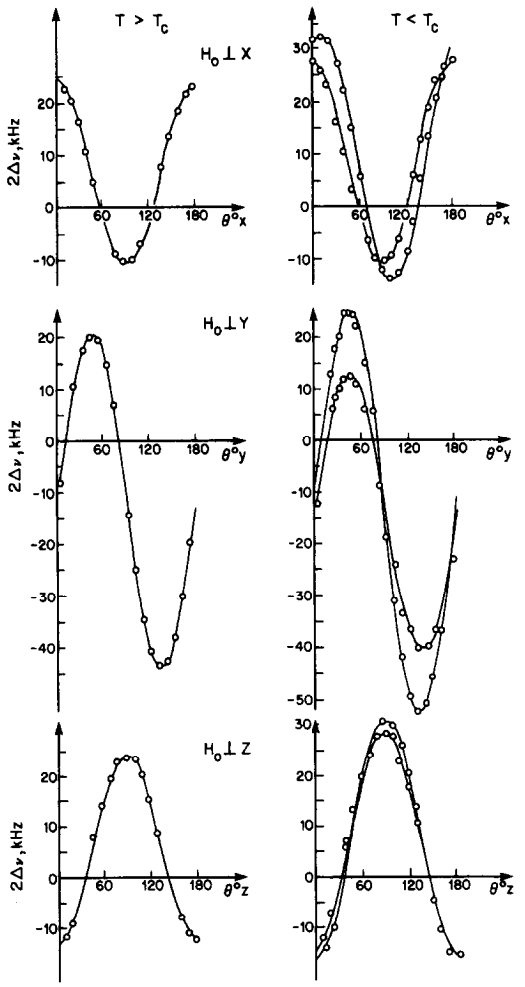

FIG. 3. Rotation patterns of the first-order quadrupole splitting of the ^{133}Cs spectra of $CsH_3(SeO_3)_2$ (the transitions $\pm\frac{3}{2} \leftrightarrow \pm\frac{1}{2}$). On the left: paraelectric phase $T = -101°C$; on the right: the antiferroelectric phase $T = -144°C$. The designations of the θ angles are the same as in Fig. 1.

symmetric and contains four Cs^+ ions, but only two of them are crystallographically nonequivalent. The gradual change of the EFG tensor in the paraelectric phase, the distortion of the structure at the transition in the antiferroelectric phase, and the establishment of an ordered state in the range 30° below T_c are followed from the temperature dependence of the ^{133}Cs spectra splitting (Fig. 3). Changes of the principal values and direction cosines of the EFG tensor at the phase transition (Table III) indicate distortion of the Cs^+ and SeO_3^- network.

Discussion

The disordered structure of the paraelectric phase of CTHS crystals is reliably enough determined. The diffraction methods give a well resolved peak on each side of the center of symmetry in hydrogen bonds O(*i*) . . . O(*i*)'. The deuteron quadrupole coupling constant values on the other hand indicate noncentral and there-

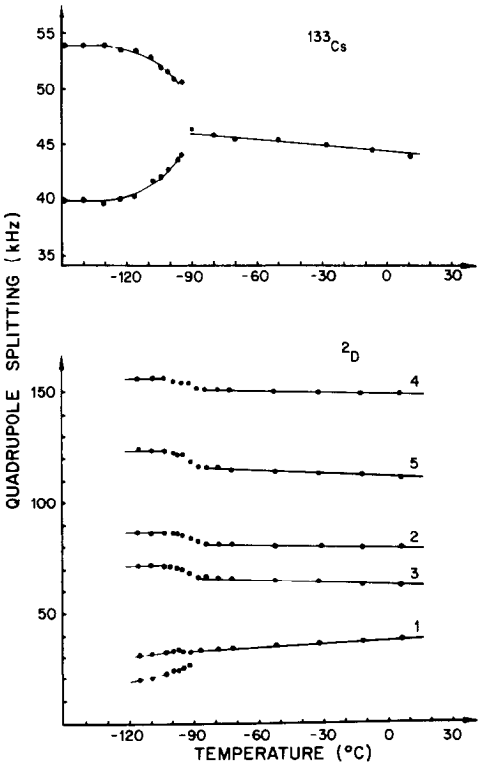

FIG. 4. Temperature dependences of the quadrupole splitting of the ^{133}Cs and ^2D spectra of $CsD_3(SeO_3)_2$. ^{133}Cs spectra splitting was measured with magnetic field $H_0 \perp Y$ and $\theta_y = 140°$ (Fig. 3); ^2D spectra splitting was measured with magnetic field $H_0 \perp X$ and $\theta_x = 68°$ (Fig. 1a).

fore disordered deuteron arrangement in these bonds. At the same time, the character of the disorder and the mechanism of the transition into the ordered phase are not clear. Static disorder is proposed in [2–5]. This assumption was first reported by Khanna in his ir study of the phase transition of CTHS. Sato and Tellgren and coworkers supported this model. They described the crystal cell of CTHS as being composed of hydrogen-bonded chains of statistically distributed H_2SeO_3 molecules and $HSeO_3^-$ ions resulting in a disordered structure. However, static disorder is not argued for sure in ferroelectric order–disorder and the microscopic mechanism of such transitions into an ordered phase is not clear.

In well-known H-bonded crystals undergoing an order–disorder transition, such as KDP, $NaH_3(SeO_3)_2$, $KH_3(SeO_3)_2$, and others, the disorder is dynamic and is accompanied by rapid jumping of hydrogens from one equilibrium site in the H bond to another. When the temperature is decreased through T_c, the jumping motions of the protons are frozen, resulting in protons ordered in one of the equilibrium sites. Such type disorder was confirmed by incoherent neutron scattering [9, 10] as well as by DMR [11–13] measurement of these crystals. Some properties of the CTHS crystals may show evidence of dynamic disorder. The large isotopic effect indicates that the role of proton dynamics in the phase transition may be important as in the case of KH_2PO_4. The lengthening of the disordered H bonds on going to the antiferroelectric phase of CTHS equals 0.032–0.038 Å (Table II) and is the same as that found from ND data in KDP crystals [14].

The DMR method has a possibility in principle of distinguishing between dynamic and static disorder in case of a double-minimum type potential. Such conclusions is based on analyses of the directions of the principal axes of the deuteron EFG tensor. The direction of the q_{vv} axis is nearly perpendicular to the Se–O . . . O plane. From analysis of the φ_v angles between q_{vv} and the normal to the Se–O . . . O plane, one can determine which of the two oxygen atoms the hydrogen atom is attached to. When the hydrogen atom is jumping back and forth between equilibrium positions of a double-minimum potential with a rapid rate (usually of the order of 10^5Hz), the observed q_{vv} axis direction is approximately the bisector of the angle between the two plane normals. In CTHS crystals the O(i) . . . O(i)′ hydrogen bonds cross the symmetry centers and the EFG tensor of the D(2)–D(5) deuterons must be the same when these deuterons are covalently bonded to O(i) or O(i)′ or dynamically disordered in a double-minimum potential. Therefore, the DMR results will be the same for dynamic and static disorder and, from static deuteron EFG measurements only, it is not possible to determine the disorder character.

The data on the hydrogen bond network in the ordered phase (their lengths and directions with respect to the X, Y, Z axes) are obtained in this work for the first time and are given in Tables I and II. The hydrogen bond network changes little on going through the Curie point. The disordered H bonds are lengthened by 0.03–0.04 Å and ordered H bonds are shortened by 0.02–0.03 Å below T_c. The changes of the directions of the H bonds are 3–4° for D(1) sites and 1–2° for D(2)–D(5) sites. These changes may be caused by slight rotation of the SeO_3 groups.

One can suggest the next mechanism of the phase transition. In the paraelectric phase, the deuterons D(2)–D(5) are disordered and disorder is rather dynamical and connected with the deuteron motion in the two-minimum potential well. Below T_c this motion is frozen and deuterons are fixed in one minimum. The paraelectric unit cell loses the symmetry center and is doubled in

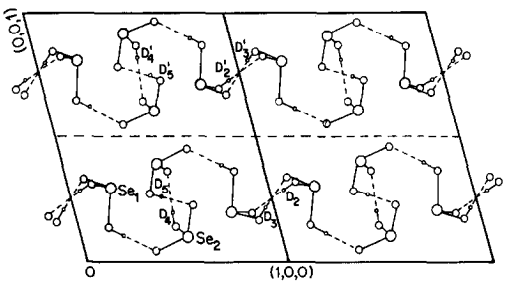

FIG. 5. Proposed hydrogen bond network and deuteron arrangement in the antiferroelectric phase of $CsD_3(SeO_3)_2$.

the c direction. Order–disorder of the hydrogen bond system is followed by distortion of the heavy-ion system. Appearance of two nonequivalent Cs sites and two nonequivalent O(1) . . . O(6) hydrogen bonds is connected with the ordering. At the same time, the O(i) . . . O(i)′ hydrogen bonds remain equivalent in the ordered unit cell because this cell has a centre of symmetry [*1*, *2*] and D(i) and D(i)′ sites are centrosymmetrically related. Such an arrangement of deuterons causes the dipoles which are ordered alternately to cancel one another, resulting in antiferroelectric behavior. On the base of this model, Fig. 5 shows schematically the structure of the low-temperature phase and the arrangement of the deuterons. The structure consists of $DSeO_3^-$ ions and D_2SeO_3 molecules, bound by hydrogen bonds. The $Se(1)O_3$ groups transform into D_2SeO_3 molecules and the $Se(2)O_3$ groups transform into $DSeO_3$ ions.

References

1. Y. MAKITA, *J. Phys. Soc. Japan* **20**, 1567 (1965).
2. S. SATO, *J. Phys. Soc. Japan* **32**, 1670 (1972).
3. R. TELLGREN AND R. LIMINGA, *Ferroelectrics* **8**, 629 (1974).
4. S. CHOMNILPAN, R. TELLGREN, AND R. LIMINGA, *Acta Crystallgr. Sect. B* **34**, 373 (1978).
5. R. K. KHANNA, M. HORAK, AND E. R. LIPPICOTT, *J. Chem. Phys.* **45**, 982 (1966).
6. G. V. GAVRILOVA-PODOLSKAYA, M. L. AFANASJEV, A. G. LUNDIN, AND A. L. JUDIN, *Izv. Akad. Nauk SSSR, Ser. Fiz.* **31**, 1108 (1967).
7. G. M. VOLKOFF, H. E. PETCH, AND D. W. L. SMELLIE, *Can. J. Phys.* **30**, 270 (1953).
8. G. SODA AND T. CHIBA, *J. Phys. Soc. Japan* **26**, 249 (1969).
9. J. PALACIOS AND U. BUCHENAU, *Ferroelectrics* **25**, 565 (1980).
10. H. GRIMM, H. STILLER, AND TH. PLESSER, *Phys. Status Solidi* **42**, 207 (1970).
11. J. L. BJORKSTAM AND E. A. UEHLING, *Phys. Rev.* **114**, 961 (1959).
12. R. BLINC, J. STEPISNIK, AND I. ZUPANCIC, *Phys. Rev.* **176**, 732 (1968).
13. M. KASAHARA, *J. Phys. Soc. Japan* **44**, 537 (1978).
14. G. E. BACON AND R. S. PEASE, *Proc. Roy. Soc.* **230**, 359 (1955).